



ChemComm

Enhanced Circularly Polarized Luminescence Dissymmetry of [Ru(bpy)₃]²⁺ Complexes in a 3D Chiral Framework: A Study of Transparent Thin Films

Journal:	<i>ChemComm</i>
Manuscript ID	CC-COM-08-2023-004083.R1
Article Type:	Communication

SCHOLARONE™
Manuscripts

COMMUNICATION

Enhanced Circularly Polarized Luminescence Dissymmetry of $[\text{Ru}(\text{bpy})_3]^{2+}$ Complexes in a 3D Chiral Framework: A Study of Transparent Thin Films

Received 00th January 20xx,
Accepted 00th January 20xx

Songwei Zhang^a, David Schnable^b, Jocelyn Elgin^a, Gaël Ung^{*b}, and Yiyang Wu^{*a}

DOI: 10.1039/x0xx00000x

Circularly polarized luminescence (CPL) plays an important role in the development of advanced optical devices. However, the design of CPL-active materials with a decent dissymmetry factor is still challenging. Here, we report CPL-active transparent thin films made from optically active ruthenium complexes $[\text{Ru}(\text{bpy})_3]^{2+}$ embedded in chiral inorganic frameworks. Due to the unique chiral-in-chiral combination, the obtained $[\text{Ru}(\text{bpy})_3][\text{Zn}_2(\text{C}_2\text{O}_4)_3]$ displays CPL activity with a dissymmetry factor of 5×10^{-3} . The CPL measurements show that the luminescence dissymmetry factor can be effectively enhanced by one order of magnitude when optically active $[\text{Ru}(\text{bpy})_3]^{2+}$ complex is incorporated into a chiral inorganic framework compared to its solution form. This study not only emphasize the potential of constructing CPL-active thin films with coordination polymers but also points out the importance of introducing extra chiral environment to improve the CPL effect.

Of the different types of polarized light, circularly polarized light is particularly significant, as it holds some important applications in the design of sensors, three-dimensional imaging, and optical information storage^{1–3}. A primary challenge of developing circularly polarized luminescent (CPL) materials is achieving a large luminescence dissymmetry factor (g_{lum}), which is a measure of the degree of circular polarization, where $g_{\text{lum}} = 2 \times (I_L - I_R) / (I_L + I_R)$. Here, I_L and I_R refer to the intensity of left-handed and right-handed circularly polarized emissions, respectively. The range of g_{lum} is between -2 and 2 which indicates a complete right or left circular polarization. In most cases, the design of CPL materials requires the molecules to contain both chiral and luminescent units. Until now, the synthesis procedures for most chiral organic emitters have been complicated and mainly relied on a few of organic derivatives,

or some dye molecules covalently bonded with chiral molecules with a relatively small g_{lum} factor ($\sim 10^{-2}$ to 10^{-5})^{4–6}. Therefore, many approaches, such as supramolecular self-assemblies of emitters into chiral structures^{7–12}, have been proposed to amplify g_{lum} values and expand the family of materials with CPL properties. However, most of these organic emitters or their super-assemblies exhibit luminescence solely in a solution state due to aggregation-induced quenching, which limits their applications.

Developing homogeneous crystalline CPL-active materials with large g_{lum} factors is promising for practical applications but remains challenging. As an emergent class of solid-state materials, chiral metal-organic frameworks (MOFs) have recently attracted lots of attentions in CPL due to their diverse structures and tunable functionalities¹³. However, MOFs with CPL remain still scarce to date due to complicated synthetic procedures of the intrinsically chiral building blocks^{14,15}. A strategy to fabricate CPL MOFs involves utilizing chiral MOFs as matrices to encapsulate guest emitters, resulting in host-guest systems^{2,14,23,15–22}, which help transfer the chirality from chiral frameworks to achiral emitters. There are several advantages of this strategy. First, the existing chiral MOFs can be directly used to host some well-reported dyes to avoid complicated synthetical design. Second, due to a confined space provided by inorganic frameworks and large separation of neighboring dye molecules, the aggregation-induced quenching effect can be effectively weakened and nonradiative relaxations can be greatly mitigated. However, in this host-guest system, the loading amount of dye molecules is limited and the details of dye molecules packing mode is difficult to resolve, which hinders the understanding of the CPL effect. As a simple bis-bidentate ligand, metal-oxalate coordination compounds have been well studied, and a series of materials with diverse structures can be generated, including one, two, three dimensional structures^{24–26}. Among them, the chiral (10,3)-a network induced by metal complexes with propeller chirality is

^a Department of Chemistry and Biochemistry, The Ohio State University, 100 West 18th Avenue, Columbus, OH 43210, USA. E-mail: wu@chemistry.ohio-state.edu

^b Department of Chemistry, University of Connecticut, 55 North Eagleville Rd., Storrs Mansfield, Connecticut 06269-3060, USA. E-mail: gael.ung@uconn.edu
Electronic Supplementary Information (ESI) available: [details of any supplementary information available should be included here]. See DOI: 10.1039/x0xx00000x

of great interest for CPL but have been rarely investigated^{24,27–31}. Very recently, Awaga and co-workers demonstrated the CPL activity of a series of enantiomerically pure $[\text{Ru}(\text{bpy})_3][\text{M}_2(\text{C}_2\text{O}_4)_3]$ ($\text{M} = \text{Zn}, \text{Mn}$) by measuring powder samples in a KBr matrix³². However, due to the difficulty of generating powder samples with reliable particle sizes and shapes, obtaining CPL results on solid-state samples that are reliable and artifact-free is challenging^{33,34}. In this work, a polyvinylpyrrolidone-assisted (PVP-assisted) synthesis method was reported to fabricate crystalline and transparent thin films of optically active (10, 3)-a coordination polymers, $[\text{Ru}(\text{bpy})_3][\text{Zn}_2(\text{C}_2\text{O}_4)_3]$ for CPL measurements. The films displayed CPL signals with an enhanced g_{lum} factor of 5×10^{-3} compared to $[\text{Ru}(\text{bpy})_3]^{2+}$ solutions.

$[\Lambda\text{-Ru}(\text{bpy})_3][\text{Zn}_2(\text{C}_2\text{O}_4)_3]$ and $[\Delta\text{-Ru}(\text{bpy})_3][\text{Zn}_2(\text{C}_2\text{O}_4)_3]$ were synthesized from the corresponding enantiopure $[\Lambda\text{-Ru}(\text{bpy})_3]^{2+}$ or $[\Delta\text{-Ru}(\text{bpy})_3]^{2+}$ salts prepared by a previously-reported diastereomeric recrystallization method³⁵. $[\Lambda/\Delta\text{-Ru}(\text{bpy})_3][\text{Zn}_2(\text{C}_2\text{O}_4)_3]$ crystallized in the space groups of $P4_132$ or $P4_332$, which contains a 3-connected (10,3) oxalate-based anionic framework, $[\text{Zn}_2(\text{C}_2\text{O}_4)_3]^{2-}$ and cationic metal complexes, $[\text{Ru}(\text{bpy})_3]^{2+}$. In the structure, neighboring Zn^{2+} ions are bridged by the bis-(bidentate) oxalate ligands along all three dimensions. This generates a polymeric framework, while the $[\text{Ru}(\text{bpy})_3]^{2+}$ cations are situated within the spacious cavity of this framework, as shown in **Figure 1**. The local configuration between neighboring chiral hexacoordinated metal centers governs the framework's dimensionality. Taking the crystal structure of $[\Lambda\text{-Ru}(\text{bpy})_3][\text{Zn}_2(\text{C}_2\text{O}_4)_3]$ as an example, the enantiopure $\Lambda\text{-}[\text{Ru}(\text{bpy})_3]^{2+}$ induces a chiral arrangement of the prochiral Zn centers into homochiral bridging of $\Lambda\text{-Zn}$ centers leading to a three dimensional chiral network. Overall, both the homochiral arrangement of the inorganic framework,

$[\text{Zn}_2(\text{C}_2\text{O}_4)_3]^{2-}$ and the packing of organic complex, $[\text{Ru}(\text{bpy})_3]^{2+}$ display a helical chiral structure with a $4_1/4_3$ -screw axis.

The powder X-ray diffraction (PXRD) and the corresponding Rietveld refinement was performed to confirm the crystal structure of $[\text{Ru}(\text{bpy})_3][\text{Zn}_2(\text{C}_2\text{O}_4)_3]$. As shown in **Figure S1**, peaks show strong intensity and well-defined positions, and the single-phase refinement fitted well with the PXRD data, indicating the compound was phase-pure and highly crystalline. To fabricate transparent thin films, PVP was added during the synthesis to assist reducing particle size and dispersing individual particle. As shown in **Figure 2**, the PXRD pattern of a $[\text{Ru}(\text{bpy})_3][\text{Zn}_2(\text{C}_2\text{O}_4)_3]$ thin film displayed good crystallinity and phase purity as well. Further, scanning electron microscope

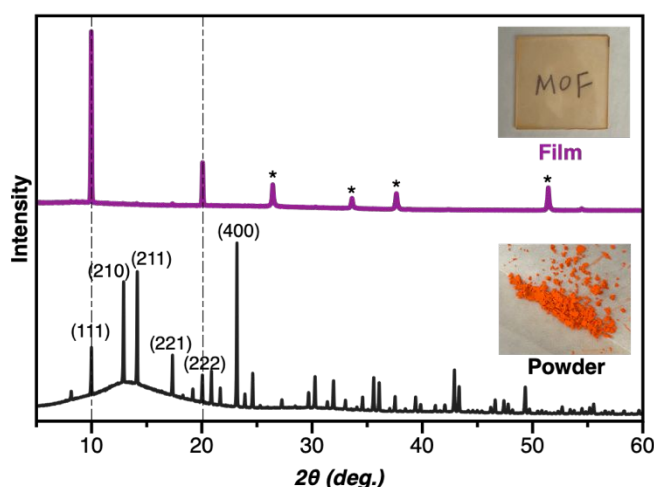


Figure 2 PXRD of $[\text{Ru}(\text{bpy})_3][\text{Zn}_2(\text{C}_2\text{O}_4)_3]$. Top: $[\text{Ru}(\text{bpy})_3][\text{Zn}_2(\text{C}_2\text{O}_4)_3]$ thin film on FTO glass (asterisk label the peaks from FTO glass substrate); Bottom: $[\text{Ru}(\text{bpy})_3][\text{Zn}_2(\text{C}_2\text{O}_4)_3]$ powder.

(SEM) was conducted on both powder and films to analyze the morphology as shown in **Figure S2**. The films exhibited smooth and homogeneous morphology, indicating the good quality.

The chirality of the $[\Lambda/\Delta\text{-Ru}(\text{bpy})_3]^{2+}$ salts and corresponding $[\Lambda/\Delta\text{-Ru}(\text{bpy})_3][\text{Zn}_2(\text{C}_2\text{O}_4)_3]$ films were confirmed by circular dichroism (CD) spectroscopy, as presented in **Figure 3**. The CD spectra exhibited one band at ~ 270 nm and several bands at ~ 450 nm with similar magnitude but opposite signs. This mirror shape indicated a pair of enantiopure films. Correspondingly, there were several strong absorption bands below 600 nm. Due to the closed shell electronic configuration for the $d^{10}\text{Zn}^{2+}$ ions, the $[\text{Zn}_2(\text{C}_2\text{O}_4)_3]^{2-}$ framework does not have $d-d$ transitions. Therefore, these absorption bands were attributed to $[\text{Ru}(\text{bpy})_3]^{2+}$ complex, which was also similar to that of $[\text{Ru}(\text{bpy})_3]^{2+}$ aqueous solution: the bands between 250 nm and 300 nm were assigned to the $\pi-\pi^*$ transitions from the bipyridine (bpy) ligands and the bands between 400 nm and 600 nm were assigned to the $d-d$ and metal-to-ligand charge transfer, MLCT ($t_{2g}-\pi^*$) transitions from $[\text{Ru}(\text{bpy})_3]^{2+}$ complex³⁶.

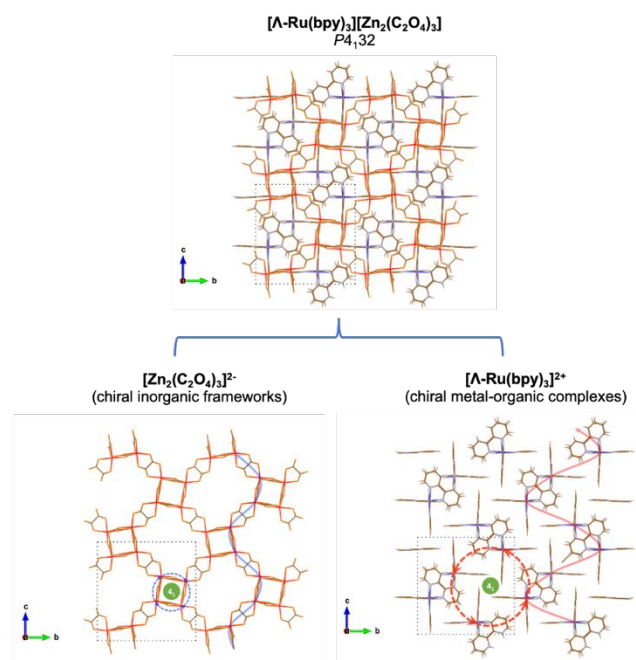


Figure 1 Crystal structure of $[\Lambda\text{-Ru}(\text{bpy})_3][\text{Zn}_2(\text{C}_2\text{O}_4)_3]$ (top): a 3-connected (10,3) oxalate-based anionic framework, $[\text{Zn}_2(\text{C}_2\text{O}_4)_3]^{2-}$ (bottom left), and a packing of cationic metal complexes, $[\text{Ru}(\text{bpy})_3]^{2+}$ (bottom right).

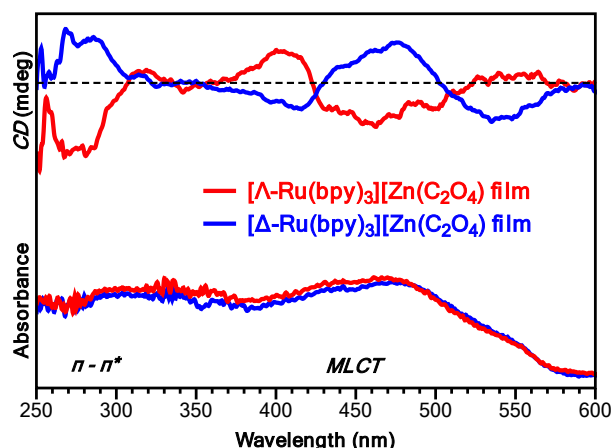


Figure 3 UV-Vis absorption spectra and CD spectra of $[\Lambda/\Delta\text{-Ru}(\text{bpy})_3][\text{Zn}_2(\text{C}_2\text{O}_4)_3]$ film on a glass substrate

To probe the CPL activity, CPL spectra (Figure 4) were measured on both $[\Lambda/\Delta\text{-Ru}(\text{bpy})_3][\text{Zn}_2(\text{C}_2\text{O}_4)_3]$ thin films and $[\Lambda/\Delta\text{-Ru}(\text{bpy})_3]^{2+}$ aqueous solutions. The total photoluminescence signal (excited at 365 nm) of $[\Lambda/\Delta\text{-Ru}(\text{bpy})_3][\text{Zn}_2(\text{C}_2\text{O}_4)_3]$ film exhibited broad emission bands centered at 580 nm, which could be assigned to a mixed $^1(\text{MLCT})$ and $^3(\text{MLCT})$ emission from $[\text{Ru}(\text{bpy})_3]^{2+}$ unit^{37,38}. The absolute value of g_{lum} factor of $[\Lambda/\Delta\text{-Ru}(\text{bpy})_3][\text{Zn}_2(\text{C}_2\text{O}_4)_3]$ was $\sim 5 \times 10^{-3}$, which was one order of magnitude larger than that of $[\Lambda/\Delta\text{-Ru}(\text{bpy})_3]^{2+}$ solutions ($\sim 6 \times 10^{-4}$) as shown in Figure S4 and S5. These results indicated that the introduction of a chiral host environment can help enhance the CPL effect from the $[\Lambda/\Delta\text{-Ru}(\text{bpy})_3]^{2+}$ complex. Based on observations in small molecules where increase rigidity improved CPL metrics, we hypothesize that this enhancement is due to the reduced molecular motion of the ligands of the Ru complexes provided by the rigid superstructure of the Zn-oxalate framework.

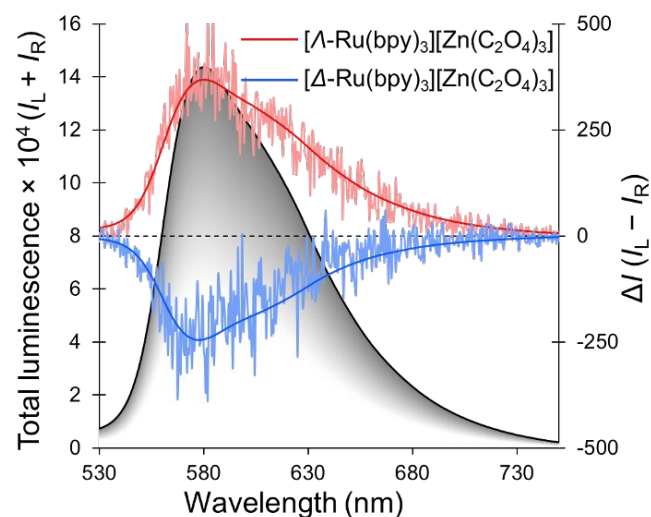


Figure 4 CPL spectra of $[\Lambda/\Delta\text{-Ru}(\text{bpy})_3][\text{Zn}_2(\text{C}_2\text{O}_4)_3]$ films on a glass substrate. The solid lines are not a fit, but a guide for the eye. See figure S3 for g_{lum} vs. wavelength plot.

Conclusions

In conclusion, we reported a PVP-assisted method to fabricate crystalline and transparent thin films of optically active (10, 3)-a coordination polymers, $[\text{Ru}(\text{bpy})_3][\text{Zn}_2(\text{C}_2\text{O}_4)_3]$ for more reliable CPL measurements. The enhanced CPL signals were observed for thin films and assigned to the introduction of a 3D homochiral environment from the inorganic building blocks.

Acknowledgments

This work is supported by Centre for Emergent Materials at The Ohio State University, a National Science Foundation (NSF) MRSEC through NSF Award No. DMR-2011876.

Conflicts of interest

There are no conflicts to declare.

Notes and references

- 1 C. Wagenknecht, C. M. Li, A. Reingruber, X. H. Bao, A. Goebel, Y. A. Chen, Q. Zhang, K. Chen and J. W. Pan, *Nat. Photonics*, 2010, **4**, 549–552.
- 2 M. Kazem-Rostami, A. Orte, A. M. Ortuño, A. H. G. David, I. Roy, D. Miguel, A. Garci, C. M. Cruz, C. L. Stern, J. M. Cuerva and J. F. Stoddart, *J. Am. Chem. Soc.*, 2022, **144**, 9380–9389.
- 3 D. Parker, J. D. Fradgley and K. L. Wong, *Chem. Soc. Rev.*, 2021, **50**, 8193–8213.
- 4 Y. Deng, M. Wang, Y. Zhuang, S. Liu, W. Huang and Q. Zhao, *Light Sci. Appl.*, 2021, **10**, 1–18.
- 5 H. Tanaka, Y. Inoue and T. Mori, *ChemPhotoChem*, 2018, **2**, 386–402.
- 6 N. Chen and B. Yan, *Molecules*, 2018, **23**(12), 3376
- 7 C. Zhang, S. Li, X. Dong and S. Zang, *Aggregate*, 2021, **2**, 1–23.
- 8 J. Kumar, T. Nakashima, H. Tsumatori, M. Mori, M. Naito and T. Kawai, *Chem. - A Eur. J.*, 2013, **19**, 14090–14097.
- 9 R. Tempelaar, A. Stradomska, J. Knoester and F. C. Spano, *J. Phys. Chem. B*, 2011, **115**, 10592–10603.
- 10 K. Ma, W. Chen, T. Jiao, X. Jin, Y. Sang, D. Yang, J. Zhou, M. Liu and P. Duan, *Chem. Sci.*, 2019, **10**, 6821–6827.
- 11 B. A. San Jose, S. Matsushita and K. Akagi, *J. Am. Chem. Soc.*, 2012, **134**, 19795–19807.
- 12 T. Zhao, J. Han, X. Qin, M. Zhou and P. Duan, *J. Phys. Chem. Lett.*, 2020, **11**, 311–317.
- 13 L. A. Hall, D. M. D'Alessandro and G. Lakhwani, *Chem. Soc. Rev.*, 2023, **52**, 3567.
- 14 X. Z. Wang, M. Y. Sun, Z. Huang, M. Xie, R. Huang, H. Lu, Z. Zhao, X. P. Zhou and D. Li, *Adv. Opt. Mater.*, 2021, **9**, 1–6.
- 15 S. M. Chen, L. M. Chang, X. K. Yang, T. Luo, H. Xu, Z. G. Gu and J. Zhang, *ACS Appl. Mater. Interfaces*, 2019, **11**, 31421–31426.
- 16 C. Zhang, Z. P. Yan, X. Y. Dong, Z. Han, S. Li, T. Fu, Y. Y. Zhu, Y. X. Zheng, Y. Y. Niu and S. Q. Zang, *Adv. Mater.*, 2020, **32**,

- 1–11.
- 17 T. Zhao, J. Han, Y. Shi, J. Zhou and P. Duan, *Adv. Mater.*, 2021, **33**, 1–10.
- 18 Y. H. Xiao, P. Weidler, S. S. Lin, C. Wöll, Z. G. Gu and J. Zhang, *Adv. Funct. Mater.*, 2022, **32**, 1–9.
- 19 C. Li, H. Schopmans, L. Langer, S. Marschner, A. Chandresh, J. Bürck, Y. Tsuchiya, A. Chihaya, W. Wenzel, S. Bräse, M. Kozłowska and L. Heinke, *Angew. Chem.* **2023**, 135, e202217377.
- 20 R. Zhai, Y. Xiao, Z. Gu and J. Zhang, *Nano Res.*, 2022, **15**, 1102–1108.
- 21 Y. Tang, W. He, Y. Lu, J. Fielden, X. Xiang and D. Yan, *J. Phys. Chem. C*, 2014, **118**, 25365–25373.
- 22 H. Chen, Z. G. Gu and J. Zhang, *J. Am. Chem. Soc.*, 2022, **144**, 7245–7252.
- 23 L. Hu, K. Li, W. Shang, X. Zhu and M. Liu, *Angew. Chemie - Int. Ed.*, 2020, **59**, 4953–4958.
- 24 S. Decurtins, H. W. Schmalle, P. Schnewly, J. Ensling and P. Gütllich, *J. Am. Chem. Soc.*, 1994, **116**, 9521–9528.
- 25 E. Coronado, J. R. Galá N-Mascaró and C. Martí-Gastaldo, *J. Am. Chem. Soc.* 2008, **130**, 14987–14989
- 26 S. Natarajan. *Solid State Sciences*. 2002, **4**, 1331-42.
- 27 E. Coronado, J. R. Galán-Mascarós, C. J. Gómez-García and J. M. Martínez-Agudo, *Inorg. Chem.*, 2001, **40**, 113–120.
- 28 A. Dikhtiarenko, P. Villanueva-Delgado, R. Valiente, J. R. García and J. Gimeno, *Polymers (Basel)*, 2016, **8**, 1–20.
- 29 F. Pointillart, C. Train, M. Gruselle, F. Villain, H. W. Schmalle, D. Talbot, P. Gredin, S. Decurtins and M. Verdaguer, *Chem. Mater.*, 2004, **16**, 832–841.
- 30 M. Brissard, M. Gruselle, C. Train, J. Vaissermann, B. Male, J. Jamet, M. Verdaguer, M. Curie, P. Cedex, L. De, P. Solides and R. April, *Inorg. Chem.*, 2001, **40**, 4633–4640
- 31 J. Habjanič, M. Jurić, J. Popović, K. Molčanov and D. Pajić, *Inorg. Chem.*, 2014, **53**, 9633–9643.
- 32 K. Nakashima, R. Suizu, S. Morishita, N. Tsurumachi, M. Funahashi, H. Masu, R. Ozawa, K. Nakamura and K. Awaga, *ACS Mater. Au*, 2023, **3**, 201–205
- 33 G. Longhi, E. Castiglioni, J. Koshoubu, G. Mazzeo, S. Abbate, *Chirality*, 2016, **28**, 696-707.
- 34 X. Liu and R. Jin, *Chem. Synth.*, 2022, **2**, 7.
- 35 F. H. Burstall, *J. Chem. Soc.*, 1936, 173-175
- 36 A. Dikhtiarenko, P. Villanueva-Delgado, R. Valiente, J. R. García and J. Gimeno, *Polym.*, 2016, **8**, 48.
- 37 A. C. Bhasikuttan, M. Suzuki, S. Nakashima and T. Okada, *J. Am. Chem. Soc.* 2002, **124**, 8398–8405.
- 38 A. Cannizzo, F. Van Mourik, W. Gawelda, G. Zgrablic, C. Bressler, M. Chergui, [A Cannizzo, F. Van Mourik, W. Gawelda, G. Zgrablic, C. Bressler and M. Chergui, *Angew. Chem. Int. Ed*, 2006, **45**, 3174–3176.